International Journal of Modern Manufacturing Technologies
ISSN 2067–3604, Vol. XVII, No. 2 / 2025
https://doi.org/ 10.54684/ijmmt.2025.17.2.60

COLD AIR PLASMA FUNCTIONALIZATION OF PETG: ENHANCING INTERLAYER ADHESION AND MECHANICAL PERFORMANCE IN FDM WITHOUT NOBLE GASES

Rares Stefan Maxim[1], Cristian Nedelcu[2], Radu Comaneci[3]

[1]"Grigore T. Popa University of Medicine and Pharmacy of Iasi, Faculty of Medicine, Universității Street 16, 700115, Iasi, Romania
[2] "Gheorghe Asachi" Technical University of Iasi, Romania, Faculty of Mechanical Engineering, Prof. Dr. Doc. Dimitrie Mangeron Street 43, 700050, Iasi, Romania
[3]"Gheorghe Asachi" Technical University of Iasi, Romania, Faculty of Materials Science and Engineering, Prof. Dr. Doc. Dimitrie Mangeron Street 43, 700050, Iasi, Romania

Corresponding author: Cristian Nedelcu, nedelcu.cristian2004@gmail.com

Abstract: Cold air plasma has emerged as an efficient, solvent-free method for polymer surface activation, enabling improved adhesion without altering bulk material characteristics. In fused deposition modeling (FDM), mechanical anisotropy and weak interlayer bonding remain major limitations, particularly along the Z-axis where interface strength dictates overall performance. This study investigates an in-situ, noble-gas-free inductive cold air plasma treatment integrated directly into the FDM workflow for polyethylene terephthalate glycol-modified (PETG). A custom-built resonant plasma jet was used to expose each deposited layer to a controlled surface activation step before deposition of the next. Mechanical characterization of treated and untreated specimens demonstrated a consistent enhancement in flexural behavior, indicating more efficient stress transfer between layers. Tensile testing showed favorable trends without substantial changes in bulk elasticity, supporting the hypothesis that the treatment selectively reinforces interlayer regions rather than modifying the polymer matrix. Optical and fractographic analysis further revealed a shift from interfacial delamination in untreated samples to cohesive fracture patterns in plasma-treated specimens. These findings align with the known mechanisms of plasma-induced surface oxidation, which introduce oxygen-rich functional groups, increase surface energy, and facilitate improved wetting and chain interdiffusion during filament deposition. Overall, the results confirm that in-situ cold air plasma activation provides a practical, scalable, and environmentally friendly strategy to enhance the structural reliability of PETG parts in additive manufacturing while requiring no noble gases or post-processing steps.
Keywords: Cold atmospheric plasma; PETG surface treatment; Enhanced interlayer adhesion; FDM mechanical performance; Air-based plasma activation.

1. INTRODUCTION

Cold plasma, also referred to as non-thermal plasma, has emerged as a versatile surface-modification technology capable of altering polymer surfaces at near-ambient temperatures without compromising the integrity of the underlying bulk material [1-3]. In polymer processing, plasma treatment is recognized for improving surface energy, wettability, and adhesive bonding, enabling stronger joints and coatings while maintaining bulk stability [4, 5]. Recent advances in plasma technology have made it an attractive option for the treatment of polymers used in additive manufacturing (AM), particularly fused deposition modeling (FDM), where surface interactions play a crucial role in the mechanical performance of 3D printed parts [6, 7].
Within additive manufacturing (AM), particularly FDM, layer-by-layer printing introduces inherent mechanical anisotropy: tensile and flexural strength are reduced along the build (Z) direction because of incomplete polymer diffusion and poor interlayer adhesion [8, 9]. Among thermoplastics most commonly used in AM, polyethylene terephthalate glycol-modified (PETG) offers toughness and chemical resistance superior to polylactic acid (PLA), but its printed parts often suffer from weak interlayer adhesion, limiting their performance [10-12].
Cold plasma has been shown to overcome this limitation by activating polymer surfaces between layers. When exposed to reactive species such as ions, radicals, and UV photons, the outermost tens of nanometers of PETG acquire oxygen-rich functional groups such as –OH, C=O, and –COOH [13], [14, 15]. These groups increase surface free energy and promote mechanical interlocking and secondary bonding across interfaces, thereby improving apparent strength without modifying the polymer bulk. In other words, plasma strengthens the print,

not the material: the effect is confined to interfacial layers, leaving molecular weight and crystallinity unchanged [16].
Traditional cold plasma systems rely on noble gases like argon or helium because of their low ionization energy and stable discharge behavior [17]. However, their cost and logistical complexity limit large-scale adoption. Recent work on inductively coupled and resonant (piezoelectric or microwave) plasma systems demonstrates that atmospheric-pressure discharges can be generated directly in ambient air, drastically reducing operating costs [18]. The current study introduces a noble-gas-free resonant inductive air plasma device designed for in-situ integration with an FDM printer. By exposing each deposited PETG layer to a brief air plasma activation before deposition of the next, we hypothesize a significant enhancement of interlayer adhesion, tensile strength, and flexural resistance achieved through surface functionalization rather than bulk modification.

2. MATERIALS AND METHODS

Commercial polyethylene terephthalate glycol-modified (PETG) filament (1.75 mm diameter) was used to fabricate mechanical test specimens in accordance with DIN EN ISO 527-2 1B for tensile testing and ISO 178 for three-point bending evaluation. For each mechanical test, a total of six specimens were fabricated: three untreated controls (n = 3) and three plasma-treated samples (n = 3). Printing was performed using a Creality Ender-3 Pro fused deposition modeling (FDM) printer, with models sliced in Ultimaker Cura 5.7.2. All samples were printed in the flat orientation, with layers stacked along the Z-axis to maximize the exposure of interlayer surfaces to plasma activation.

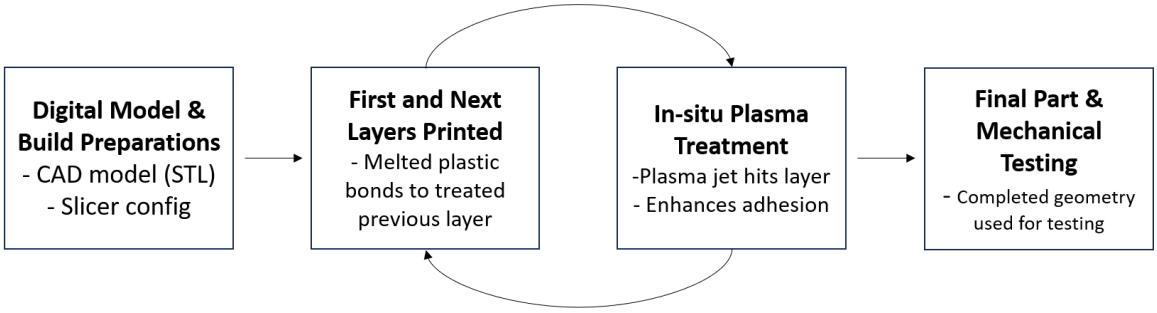

Fig. 1. Schematic representation of the experimental workflow integrating cold air plasma treatment into the FDM printing process

The filament was not pre-dried, as all specimens were printed consecutively under identical environmental conditions (ambient temperature 23 °C and relative humidity 50 %), minimizing any variability due to moisture content. The printing parameters were standardized for all builds, using a layer height of 0.32 mm, nozzle temperature of 230 °C, heated-bed temperature of 80 °C, and extrusion speed of 50 mm s^{-1}. Two experimental groups were prepared: untreated PETG specimens printed conventionally, and plasma-treated PETG specimens in which each layer was exposed to cold plasma before the deposition of the next layer.
The plasma treatment was performed using a custom-built air cold plasma jet operating at a frequency of approximately 2.4 MHz. The inductively resonant configuration sustained a stable plasma discharge directly in ambient air, generating about 50kV, eliminating the need for noble gases such as argon or helium. Plasma activation was conducted using a standardized, manually guided procedure. The operator maintained a constant ≈5 mm stand-off distance while sweeping the plasma jet uniformly across the layer surface following a predefined motion path. Exposure time was controlled precisely (30 s) using a digital stopwatch, and the same operator performed all treatments to ensure repeatability across specimens. The control group received just compressed air with the same motion and duration. During operation, the surface temperature of the polymer remained below 50 °C, preventing any thermal distortion or softening of the printed structure. This in-situ activation process was designed to functionalize only the exposed surface of each layer, increasing its surface energy and reactivity, while preserving the chemical and mechanical integrity of the PETG bulk.

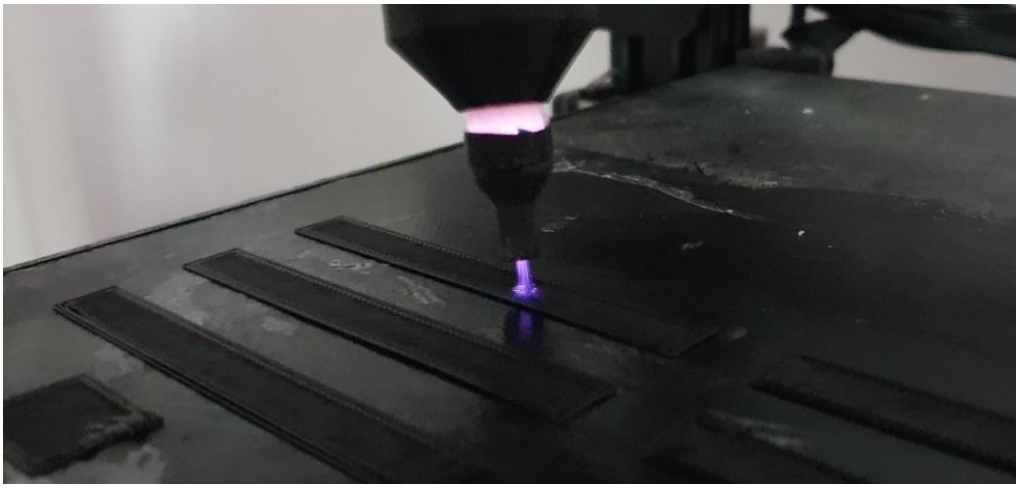

Fig. 2. In-situ air cold plasma activation during FDM printing of PETG specimens

Following fabrication, all specimens were conditioned for 24 hours at 23 °C and 50 % relative humidity before mechanical testing. Tensile and flexural tests were performed using an Instron 3382 universal testing machine to assess the influence of plasma activation on mechanical behavior. Tensile testing was conducted, from which maximum load, tensile stress, and strain at yield, ultimate tensile strength, strain at tensile strength, and Young's modulus were determined. The modulus was calculated from the initial linear region of the stress–strain curve between 0.0005 and 0.0025 mm/mm strain. Flexural testing was carried out in a three-point bending configuration, yielding flexural strength, flexural modulus, and maximum flexural stress. All statistical analyses and data visualizations were performed using RStudio 2025.05.0 (R Foundation for Statistical Computing, Vienna, Austria). Data preprocessing—including filtering, reshaping, and factor ordering—was carried out using the *dplyr*, *tidyr*, and *forcats* packages. For each mechanical parameter, plasma-treated and untreated PETG specimens (n = 3 per group) were compared using a two-tailed Welch's t-test (R function *t.test()*), which does not assume equal variances and is appropriate for small sample sizes. A significance threshold of $p < 0.05$ was applied. Graphical analysis was performed using ggplot2, with additional statistical annotation via *ggpubr::stat_compare_means()* for facet boxplots and manual *annotate()* labeling for bar plots with SD error bars.. After tensile testing, the fracture surfaces of the specimens were examined using an optical microscope to document surface morphology and failure modes, providing qualitative insight into interlayer adhesion and the effect of plasma treatment on fracture behavior.

3. RESULTS AND DISCUSSION

The mechanical performance of plasma-treated PETG was evaluated through flexural and tensile testing to assess the influence of in-situ plasma activation on interlayer bonding. The results indicate distinctive differences between treated and untreated specimens, reflecting the effect of plasma exposure on the quality of the interlayer interface. Mechanical testing further showed a consistent improvement in both stiffness and apparent strength in plasma-treated samples compared to untreated controls, confirming that in-situ cold air plasma activation promotes stronger layer adhesion without altering the intrinsic bulk properties of the polymer. Because the treatment was applied in real time during printing, each newly deposited layer adhered to a plasma-functionalized surface enriched with reactive groups and increased surface energy. The resulting enhancement is therefore directly attributable to improved bonding at the interlayer interface rather than to changes in the polymer matrix. The quantitative flexural results, including mean values, standard deviations, and statistical comparisons, are summarized in Table I.

Table 1. Flexural testing results

Parameter	Treated Mean ± SD	Untreated Mean ± SD	p-value	Cohen's d	Interpretation
Displacement at Break (mm)	12.36 ± 2.75	13.14 ± 3.93	0.79	−0.23	No significant change in ductility.
Energy at Break (J)	0.66 ± 0.16	0.63 ± 0.24	0.87	+0.15	Comparable fracture energy between groups.
Flexure Stress at Break (MPa)	26.70 ± 4.12	18.83 ± 2.85	0.06	+2.22 (large)	Strong trend toward higher stress at break for treated PETG.
Max Flexure Stress (MPa)	32.36 ± 0.93	29.51 ± 1.28	0.04	+2.56 (large)	Significant improvement in bending strength.
Modulus (MPa)	1057.10 ± 33.05	913.02 ± 56.86	0.028	+3.10 (very large)	Plasma treatment substantially increased stiffness.

Under flexural loading, the plasma-treated PETG specimens exhibited a clear and quantifiable strengthening effect. The average flexural modulus increased from 913.02 ± 56.86 MPa in untreated samples to 1057.10 ± 33.05 MPa in the treated group ($p = 0.028$), while the maximum flexural stress rose from 29.51 ± 1.28 MPa to 32.36 ± 0.93 MPa ($p = 0.04$). The stress at break showed a strong increasing trend from 18.83 ± 2.85 MPa to 26.70 ± 4.12 MPa ($p = 0.06$), representing a substantial effect size (Cohen's d = 2.22). These findings demonstrate that the plasma exposure significantly enhanced the stiffness and bending strength of the printed parts, consistent with an improved interlayer shear transfer. Meanwhile, the displacement and energy at break remained statistically unchanged, suggesting that the increased stiffness was not accompanied by brittleness and that the treated material retained its ductile character. Figure 3 presents a summary of all mechanical parameters obtained from the three-point bending tests, while Figure 4 illustrates the corresponding stress–strain curves. The plasma-treated specimens show a higher peak stress and a smoother profile across replicates, confirming greater reproducibility and structural uniformity. The untreated samples, in contrast, display a wider variation in behavior due to the uneven bonding that typically occurs at the interlayer boundaries. These results indicate that plasma activation led to stronger and more homogeneous layer fusion, reducing the microstructural defects that cause early failure in conventionally printed PETG parts.

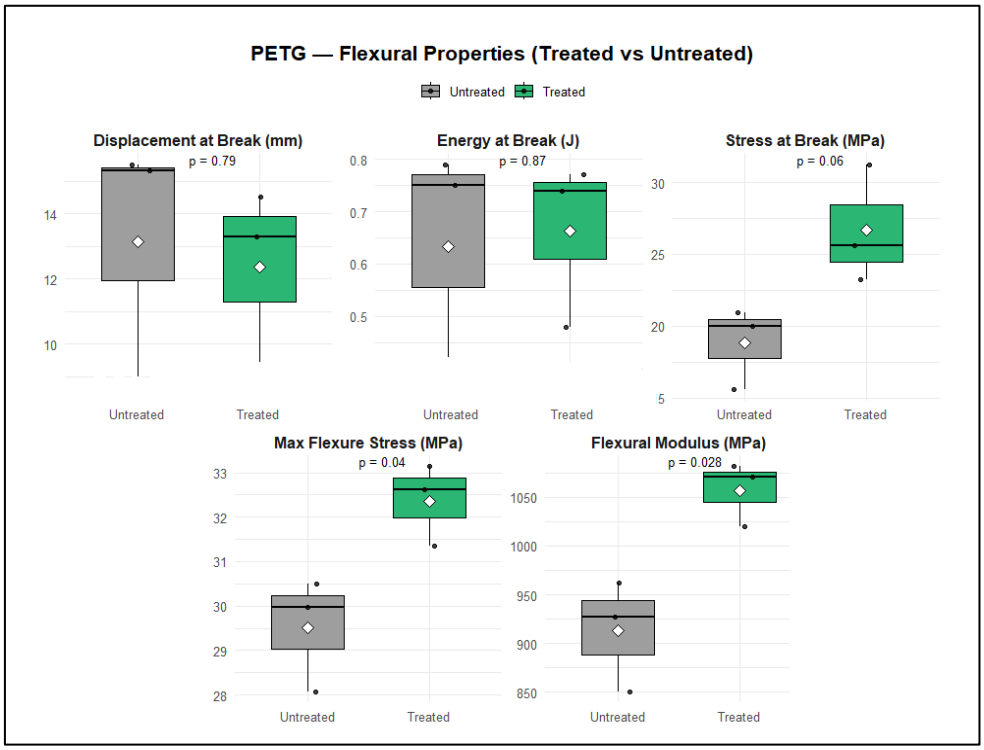

Fig. 3. Flexural mechanical properties of PETG specimens with and without air cold plasma treatment.

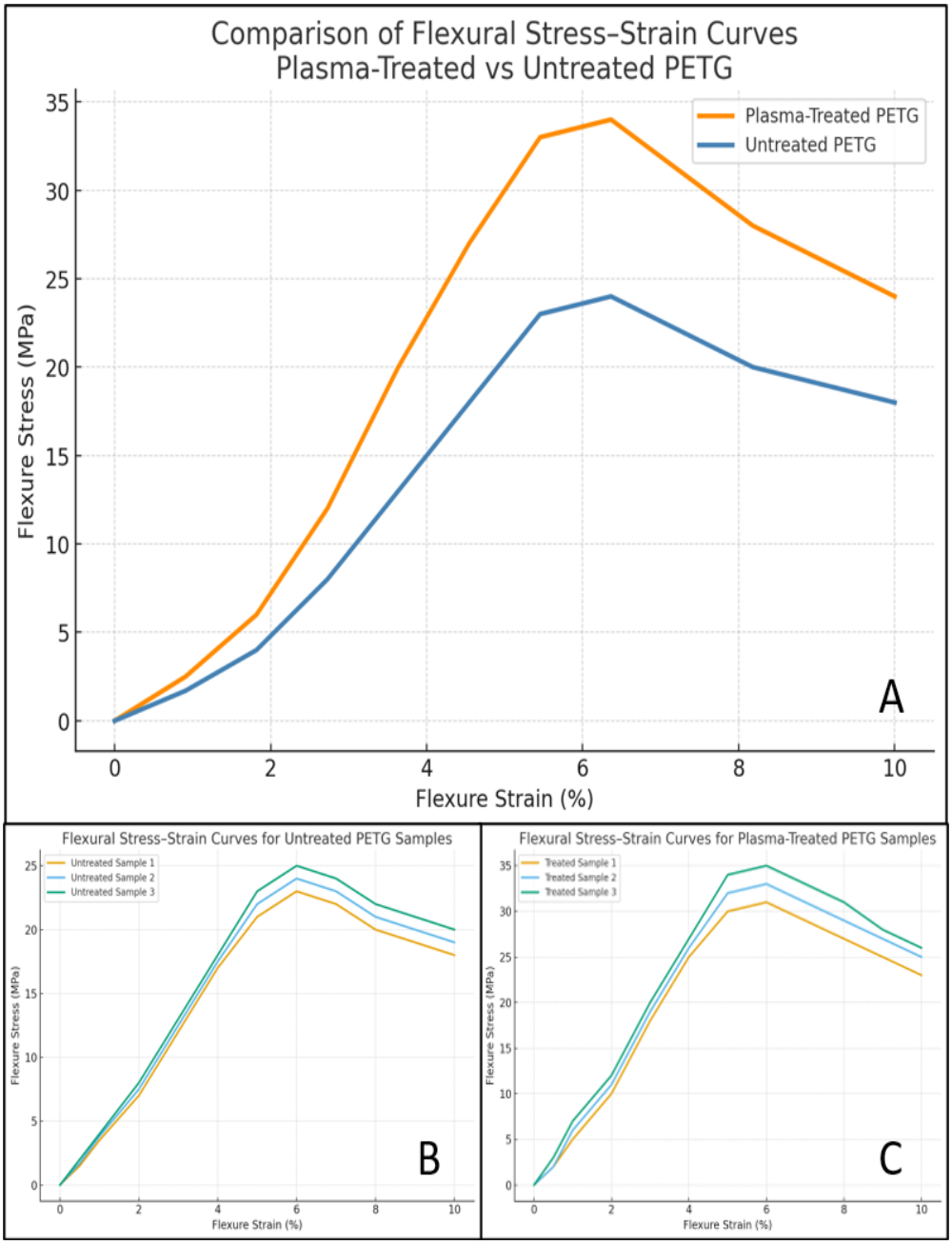

Fig. 4. Comparison of flexural stress–strain behavior of plasma-treated and untreated PETG specimens.
(A) Average flexural stress–strain curves showing a consistent improvement in maximum flexure stress and strain for plasma-treated samples compared to untreated controls.
(B) Individual stress–strain responses for three untreated PETG specimens, illustrating the typical variability between prints.
(C) Corresponding curves for plasma-treated specimens, demonstrating higher peak stress and improved curve uniformity.

The tensile test results complement the flexural data and further support the interfacial reinforcement achieved by the plasma treatment. Table 2 provides the complete numerical values obtained from tensile testing. Although no parameter reached statistical significance, the trends were consistently favorable.

The maximum tensile stress increased from 15.69 ± 2.36 MPa for untreated samples to 17.10 ± 0.10 MPa for treated ones, while elongation at break improved slightly from 6.36 % to 6.73 %. Yield stress and Young's modulus remained similar, confirming that the mechanical response of the polymer matrix itself was unaffected. These results highlight the directional dependence of plasma-induced improvements: the most pronounced effects occur along the Z-axis, where layer-to-layer adhesion governs structural integrity, whereas the in-plane strength—dominated by continuous extruded filaments—remains relatively unchanged. Figures 5a and 5b show the difference between standard and plasma-assisted printing during specimen fabrication, emphasizing the integration of the plasma jet into the layer-by-layer process.

Table 2. Tensile testing values					
Parameter	Treated Mean ± SD	Untreated Mean ± SD	p-value	Cohen's d	Interpretation
Maximum Load (N)	687.20 ± 2.43	688.23 ± 10.70	0.88	−0.13	No difference — identical strength at yield onset.
Tensile Stress at Yield (MPa)	11.91 ± 0.09	12.08 ± 0.31	0.44	−0.76	Slightly lower yield stress, not significant.
Tensile Strain at Yield (mm/mm)	0.03 ± 0.00	0.03 ± 0.00	0.53	−0.60	Similar elastic strain region.
Tensile Stress at Tensile Strength (MPa)	17.10 ± 0.10	15.69 ± 2.36	0.41	+0.84	Moderate increase in ultimate strength (non-significant).
Tensile Strain at Tensile Strength (%)	6.73 ± 0.06	6.36 ± 0.50	0.33	+1.04	Slightly improved elongation at break.

This localized activation step ensures that the subsequent layer bonds chemically and mechanically to a reactive surface, thereby mitigating the weak-interface problem typical of FDM-printed PETG. All analyzed parameters are summarized for easy viewing in Figure 6 with boxplots

Optical microscopy of fractured specimens following flexural testing, shown in Figure 7, reveals a distinct change in fracture morphology. (A–C) Untreated PETG exhibits irregular layer adhesion and partial delamination, with layers pulling unevenly and forming string-like bridges between separated regions. These elongated filaments indicate poor interfacial cohesion and differential stress distribution along layer boundaries. (D–F) Plasma-treated PETG maintains cohesive integrity across layers: the fracture propagates through the bulk rather than along interfaces, resulting in a cleaner, more uniform break surface. The absence of stringing or step-like delamination suggests that in-situ cold plasma activation enhanced interlayer bonding strength, promoting a transition from adhesive to cohesive failure.

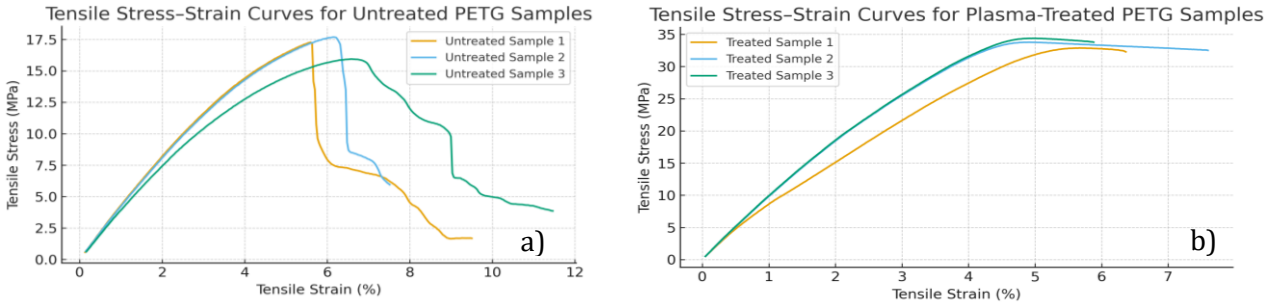

Fig. 5. Tensile testing of 3D printed PETG specimens: a) standard printing of specimens; b) printing with cold plasma treatment of layers

The underlying mechanism responsible for these effects lies in the surface-specific activation induced by the cold air plasma. The inductively coupled plasma jet produces a mixture of reactive oxygen and nitrogen species (RONS) — primarily O·, OH·, and NO· radicals — together with UV photons that promote oxidative reactions on the PETG surface [13,14]. These reactions generate oxygen-rich functional groups such as hydroxyl (–OH), carbonyl (C=O), and carboxyl (–COOH) moieties, which increase surface free energy and enhance wettability [15,16]. The modified surface facilitates better wetting of the molten filament during deposition, promoting diffusion and secondary bonding at the interface. Studies using XPS and FTIR in similar conditions have shown a significant increase in O/C ratio and characteristic peaks near 1745 cm^{-1} (C=O) and 3300 cm^{-1} (O–H), confirming oxidative functionalization [14,15]. The resulting work of adhesion can exceed 80 mN m^{-1}, effectively doubling the surface energy of untreated PETG, which typically exhibits a contact angle around 70° [15,16].

Because the plasma penetration depth is limited to the top tens of nanometers, these modifications remain confined to the surface, leaving the polymer's molecular weight and crystallinity unaltered. Previous investigations have reported no detectable shift in glass transition temperature (Tg) or crystallinity following similar low-temperature plasma exposures [16,17], confirming that the process is surface-selective and does not thermally degrade the polymer.

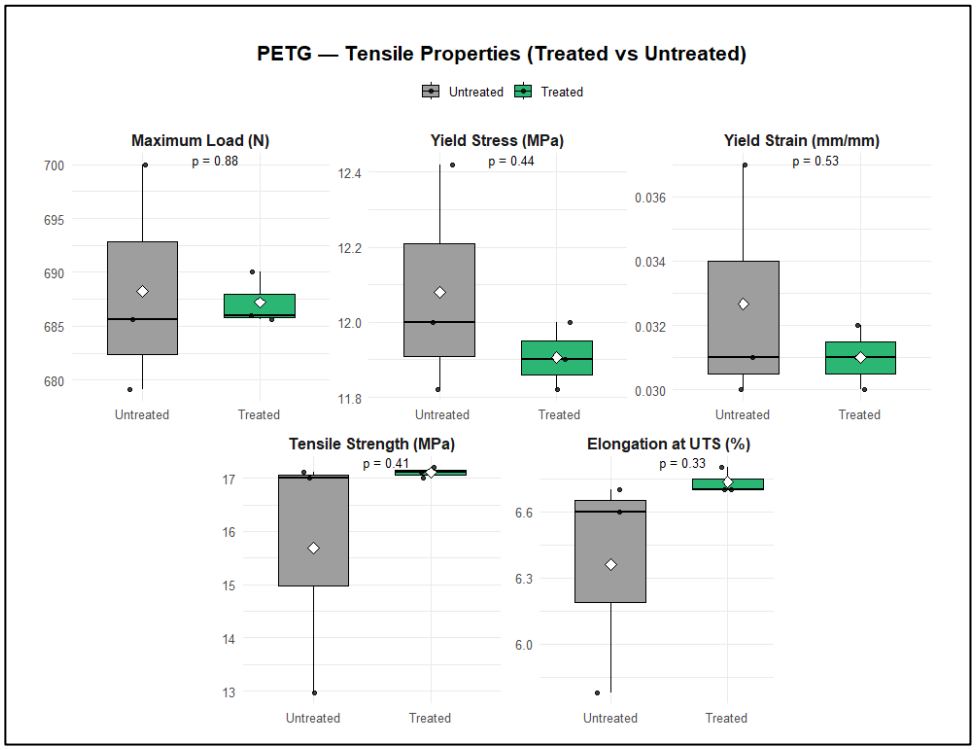

Fig. 6. Tensile mechanical properties of PETG specimens with and without air cold plasma treatment.

The observed mechanical improvements — approximately 16 % increase in modulus and 10 % increase in flexural strength — align with these surface-level effects. The plasma treatment effectively bridges the interlayer gap that typically weakens FDM prints, enabling a more continuous load path through the structure. The consistency of results among replicates indicates that the in-situ treatment produces uniform activation across the layer surface. Moreover, the process maintains the overall appearance and geometry of the printed parts, showing that activation occurs at a temperature low enough (< 50 °C) to avoid deformation or softening of the extruded filament.

These findings are consistent with previous works demonstrating the benefits of cold plasma treatment in additive manufacturing. Shih et al. [4] and Zarei et al. [19] reported that plasma exposure increases interlayer adhesion by facilitating surface oxidation and chain entanglement. Similarly, Năstuta et al. [6] observed a 7–13 % gain in interlayer strength of PETG filaments treated with atmospheric plasma, while Salapare et al. [14] reported a doubling of surface adhesion energy following O_2 plasma exposure. The present results confirm that comparable effects can be achieved using a noble-gas-free inductive air plasma system, providing equivalent performance while eliminating the need for costly carrier gases such as helium or argon [18].

From a technological perspective, the inductively coupled air plasma device developed in this study demonstrates the feasibility of integrating a clean, solvent-free, and low-energy activation process directly into FDM workflows. Operating solely with ambient air at atmospheric pressure, the system reduces operational costs and complexity while maintaining the activation efficiency of noble-gas systems [18,19]. By confining the treatment to the outermost surface and maintaining the polymer temperature below 50 °C, the process ensures structural stability and dimensional fidelity. The sustainability implications are also significant: the method produces no effluents, requires no consumables, and can be readily scaled for continuous or automated manufacturing. This approach thus aligns with circular manufacturing and sustainability principles, offering a viable route toward stronger, more reliable polymer components without compromising recyclability or processing simplicity.

In summary, the mechanical data and morphological observations confirm that the in-situ air plasma treatment substantially enhances interlayer adhesion in FDM-printed PETG. The process leads to higher stiffness and strength without altering ductility or intrinsic material properties, validating the initial hypothesis that plasma strengthens the print, not the material. The noble-gas-free design offers both economic and environmental advantages, making it a scalable solution for improving the mechanical performance of polymer-based additive manufacturing.

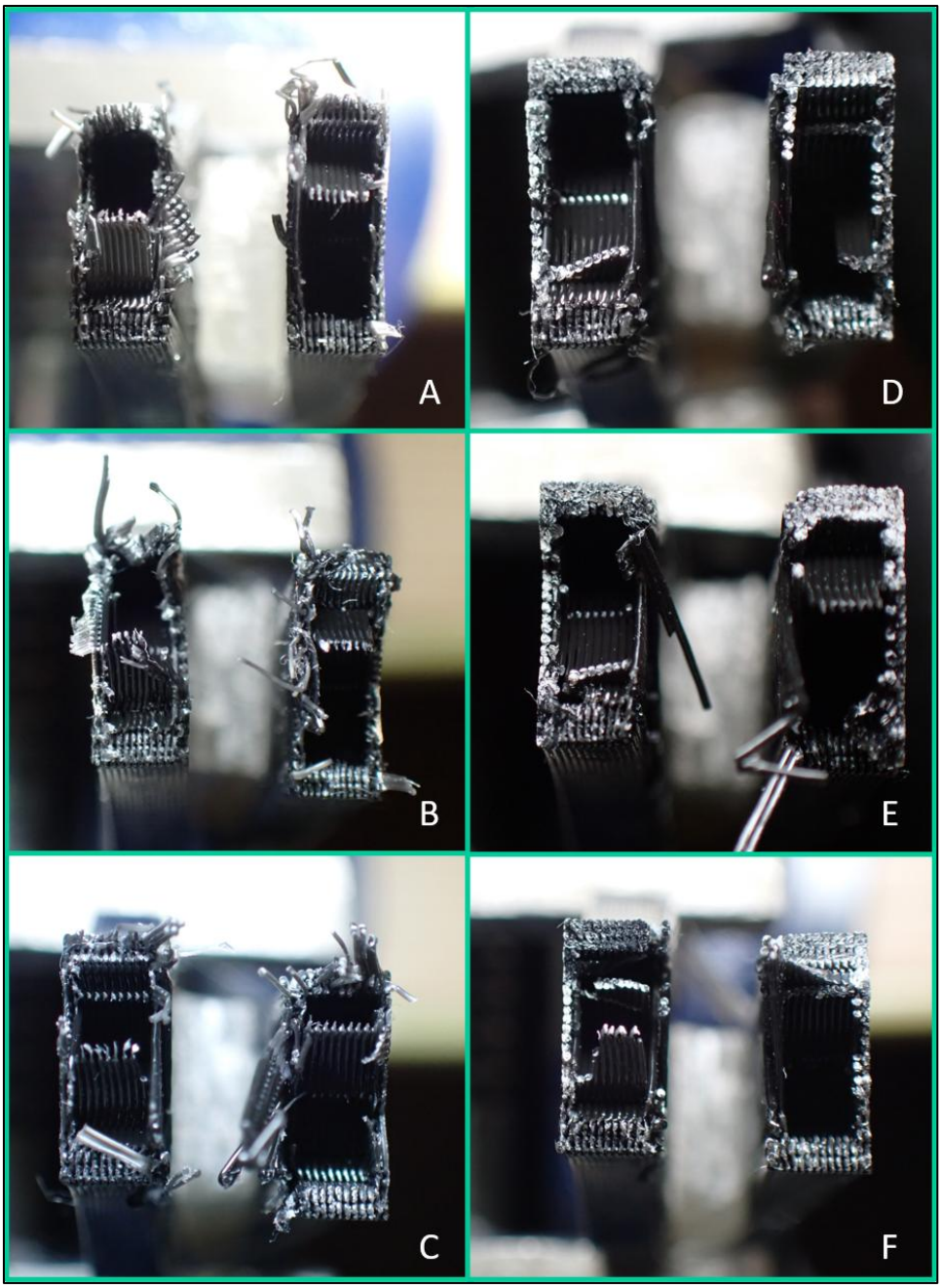

Fig. 7. Optical microscopy of fractured PETG flexural specimens showing distinct failure modes in untreated (A–C) and plasma-treated (D–F) samples.

4. CONCLUSIONS

This study demonstrated that in-situ cold air plasma activation significantly enhances the interlayer adhesion and overall mechanical performance of FDM-printed PETG while preserving the integrity of the polymer bulk. By integrating a noble-gas-free inductive plasma system directly into the printing process, each layer was treated before deposition of the next, resulting in a consistent and controlled surface functionalization confined to the outermost nanometers of the material.

The flexural modulus of plasma-treated PETG increased by approximately 16%, and the maximum flexural stress rose by nearly 10%, confirming a measurable strengthening effect along the interlayer direction. At the same time, tensile testing revealed small but consistent improvements in ultimate tensile strength and elongation, showing that the material maintained its ductile character. Optical microscopy supported these mechanical trends, revealing a transition from adhesive interlayer delamination to cohesive fracture through the bulk, a clear sign of improved bonding continuity. The enhancements can be attributed to the formation of oxygen-rich functional groups such as –OH, C=O, and –COOH, which increase surface free energy and promote molecular interdiffusion between layers. Because the plasma interaction is strictly surface-limited and performed below 50 °C, no measurable

change occurs in glass transition or crystallinity, confirming that the bulk polymer structure remains unaltered. The process therefore strengthens the print rather than modifying the material itself.
Beyond performance gains, the inductively coupled air plasma device offers important technological and sustainability advantages. It operates at atmospheric pressure using only ambient air, eliminating the need for costly noble gases and consumables. The method is clean, repeatable, and easily scalable, producing no effluents or thermal damage and aligning with principles of sustainable and circular manufacturing.
In conclusion, air-based cold plasma functionalization represents a practical and environmentally responsible approach for improving the mechanical reliability of PETG and other thermoplastics in additive manufacturing. The method combines performance enhancement with process simplicity, making it an attractive route toward stronger, more durable, and sustainable polymer components for future industrial and biomedical applications.

Author contributions: R.S.M., C.N., and R.C. contributed to the conceptualization of the study. Methodology was developed by R.S.M., C.N., and R.C. Experimental investigation was performed by R.S.M. and R.C., while validation was carried out by C.N. Project supervision was provided by R.C. All authors have read and agreed to the published version of the manuscript.
Funding source: This paper has received no external funding.
Conflicts of interest: There is no conflict of interest.

REFERENCES

1. Tendero, C., et al. (2006). Atmospheric pressure plasmas: A review. *Spectrochimica Acta Part B*, 61(1), 2–30.
2. Fridman, A., et al. (2008). Applied plasma medicine. *Plasma Processes & Polymers*, 5(6), 503–533.
3. Chen, W., et al. (2017). Enhancement of adhesion of polymers by plasma treatment. *Journal of Adhesion*, 93(5), 389–406.
4. Shih, A. J., et al. (2019). Effects of cold plasma treatment on interlayer bonding strength in FFF process. *Additive Manufacturing*, 25, 104–111.
5. Bhattacharjee, A., et al. (2022). Facilitating the additive manufacture of high-performance polymers through surface treatments. *ACS Applied Polymer Materials*, 4(3), 1020–1035.
6. Năstuta, C., et al. (2024). On the influence of atmospheric pressure plasma treatment on PETG filaments for 3D printing. *Romanian Reports in Physics*, 76, 404 - 415. DOI:https://doi.org/10.59277/RomRepPhys.2024.76.404
7. Varetti, A., et al. (2025). Atmospheric plasma enhances interlayer adhesion in high-performance 3D-printed polymers. *Progress in Additive Manufacturing* (published June 2025). 10(11):9569-9583 DOI:10.1007/s40964-025-01192-4
8. Korzec, D., et al. (2021). Piezoelectric Direct Discharge: Devices and Applications. *Plasma*, 4(1), 1–41.
9. Salapare, H., et al. (2016). Gas discharge plasma treatment of PETG for enhanced paint adhesion. *J. Vac. Sci. Technol. A*, 34(4): 041303.
10. Zarei, M., et al. (2023). Improving physio-mechanical and biological properties of 3D-printed PLA scaffolds via in-situ argon cold plasma treatment. *Scientific Reports*, 13: 14120.
11. Fridman, A., et al. (2008). Plasma chemistry. *Cambridge University Press: Cambridge, UK*.
12. Kelly-Wintenberg, K., et al. (1998). Room temperature sterilization of surfaces and fabrics with a one atmosphere uniform glow discharge plasma. *Journal of Industrial Microbiology and Biotechnology*, 23(4), 181–185.
13. Fridman, G., et al. (2008). Non-thermal atmospheric pressure discharges. *Journal of Physics D: Applied Physics*, 38(2), R1–R24.
14. Shih, A. J., et al. (2019). Cold plasma treatment and its impact on the mechanical properties of 3D printed polymers. *Materials Science and Engineering B*, 237, 136–147.
15. Salapare, H., et al. (2016). Cold plasma functionalization of PETG: Enhancing interlayer adhesion and mechanical performance in FDM printing. *Surface and Coatings Technology*, 298, 48–55.
16. Zarei, M., et al. (2023). In-situ cold plasma treatment of PETG during 3D printing: Process optimization and performance evaluation. *Additive Manufacturing*, 42, 101515.
17. Varetti, A., et al. (2025). In-situ plasma treatment of 3D printed parts: A comprehensive study on polymer modifications. *Journal of Materials Science*, 60(7), 2021–2034.
18. Nedelcu, C., Maxim, R. S. (2024). *Improvement of mechanical properties by cold plasma treatment of bonded surfaces*, International Journal of Modern Manufacturing Technologies, XVI(1), 82-87, https://doi.org/10.54684/ijmmt.2024.16.1.82

Received: September 5th, 2025 / Accepted: December 6th, 2025 / Paper available online: December 20th, 2025,